Analysis of an Arbitrarily-Shaped Planar Circuit—A Time-Domain Approach

WOJCIECH K. GWAREK

(*Invited Paper*)

***Abstract*—A study of an arbitrarily-shaped planar circuit is reported. The theoretical background is presented and then a numerical method of analysis is introduced. Experiments show good agreement between the theoretical calculations and the measurements. The examples of applications concern stripline circuits but the method may be also applied to waveguides.**

I. Introduction

THE GENERAL CONCEPT of a planar circuit was introduced by Okoshi [1] as a circuit having one dimension very small in comparison with the wavelength and an arbitrary shape in two other dimensions. The idea proved to be important from both the theoretical and the practical points of view. In microwave theory, it initiates a two-dimensional circuit theory which is an extension of the 0-dimensional lumped-element theory and one-dimensional transmission-line theory. In microwave techniques, there are a wide range of applications of the theory including the use for microwave integrated circuits.

The idea of a planar circuit leads to a mathematical problem of solving a two-dimensional Helmholtz equation for a potential V, with proper boundary conditions. To solve the problem, Okoshi and Miyoshi [1] used Weber's solution for cylindrical waves to obtain relations between the potentials on different parts of the boundary. This led to an approximate linear matrix relation which had to be solved numerically. Hsu Jui-Pang and Anada [2] have developed a method based on a set of eigenfunctions obtained numerically for a particular circuit. There were also some efforts to characterize planar elements of particular shape and to analyze a circuit composed of such elements [3], [4].

Much progress has been made and many practical problems solved; however, none of the mentioned methods seems to lead to a computer program capable of solving an arbitrarily-shaped planar circuit without an extensive theoretical and programming effort by the user. This limits their applications and justifies the search for alternative methods more practical for engineers.

All the mentioned methods, while being very different, are based on the same idea of considering only a steady-state solution for a complicated boundary problem. The idea presented in this paper is to simulate numerically the wave propagation in the structure starting from zero initial conditions. The wave propagating and reflecting from the boundaries sets up automatically the proper boundary conditions. When the steady state is reached, all the circuit parameters can be obtained.

Manuscript received February 5, 1985; revised June 3, 1985.

The author is with the Instytut Radioelektronikci, Politechnika Warszawska, Warszawa, Nowowiejska 15/19 Poland.

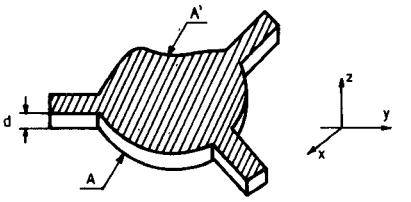

Fig. 1. A planar circuit.

II. Basic Definitions and Relations for the Considered Circuit

Hsu Jui-Pang and T. Anada [2] have presented a general circuit theory of a planar circuit extending its definition beyond the circuit of a very small height. They have based the theory on a set of E and H height modes. Their idea is followed in this paper but the formal description of the circuit is based on the Hertz potentials. This approach gives mathematical precision for the definitions and is convenient in practical use.

Let us consider the planar circuit shown in Fig. 1. The space in which the wave is transmitted is limited by two electric walls A and A' situated in the planes $z = 0$ and $z = d$. We consider two sets of modes E_n and H_n.

Definition: An E_n mode is a mode described by an electric Hertz potential π_e [5] of the form

$$\pi_e^n = \boldsymbol{a}_z \psi_e^n(x, y) \cos\left(\frac{n\pi}{d} z\right) e^{j\omega t} \tag{1}$$

where $\boldsymbol{a}_z$ is a unit vector parallel to the z-axis, and $n = 0, 1, 2, \cdots$.

An H_n mode is a mode described by a magnetic Hertz potential π_h^n of the form

$$\pi_h^n = \boldsymbol{a}_z \psi_h^n(x, y) \sin\left(\frac{n\pi}{d} z\right) e^{j\omega t} \tag{2}$$

where $n = 1, 2, \cdots$.

0018-9480/85/1000-1067$01.00 ©1985 IEEE

From the general properties of the Hertz potentials [5], we obtain for an E_n mode

$$E_z = \psi_e^n(x, y)\cos\left(\frac{n\pi}{d}z\right)\beta_t^2 e^{j\omega t}$$

$$\boldsymbol{E}_t = -\frac{n\pi}{d}\sin\left(\frac{n\pi}{d}z\right)\nabla\psi_e^n(x, y)e^{j\omega t}$$

$$H_z = 0$$

$$\boldsymbol{H}_t = -j\omega\epsilon\boldsymbol{a}_z \times \nabla\psi_e^n(x, y)\cos\left(\frac{n\pi}{d}z\right)e^{j\omega t} \tag{3}$$

where

$$\beta_t^2 = \omega^2\mu\epsilon - \left(\frac{n\pi}{d}\right)^2.$$

The surface current which flows in the upper plane A' is equal to

$$\boldsymbol{J}_e = -\boldsymbol{a}_z \times \boldsymbol{H}_t|_{z=d} = j\omega\epsilon\nabla\psi_e^n(x, y)e^{j\omega t}. \tag{4}$$

Let us define a potential

$$V_e = -d\psi_e^n(x, y)\beta_t^2 e^{j\omega t}. \tag{5}$$

Using the above relations and taking into consideration that the potential (1) satisfies the Helmholtz equation, we obtain the relations between $\boldsymbol{J}_e$ and V_e

$$\nabla V_e = -j\frac{\beta_t^2}{\omega\epsilon}d\boldsymbol{J}_e \tag{6}$$

$$\nabla\cdot\boldsymbol{J}_e = -j\frac{\omega\epsilon}{d}V_e. \tag{7}$$

In the case of an H_n mode, we obtain the formulas dual to (3), (4), and (5). These formulas include a magnetic current $\boldsymbol{J}_h$ and a magnetic potential V_h, which are related by the equations

$$\nabla V_h = -j\frac{\beta_t^2}{\omega\mu}d\boldsymbol{J}_h \tag{8}$$

$$\nabla\cdot\boldsymbol{J}_h = -j\frac{\omega\mu}{d}V_h. \tag{9}$$

There is a following correspondence between the defined modes and the popular transmission lines.

1) Stripline may be considered as a composition of two planar structures with E_0 modes. The fringing fields may be included in the calculations by extending the real dimensions of the circuit in the xy-plane by a value of [1]

$$\delta = 2d(\log_e 2)/\pi. \tag{10}$$

2) Microstrip is basically a planar structure with an E_0 mode, but the complicated nature of its fringing fields makes its analysis a more difficult problem than in the case of stripline.

3) H_{01} rectangular waveguide situated with the E field parallel to the z-axis of Fig. 1 may be considered as a planar circuit of E_0 mode with the short-circuit boundary conditions on the sides of the guide. In this case, the planar circuit methods solve the problem of a guide with changing width. When the guide is turned by $\pi/2$, it becomes a planar circuit of an H_1 mode with open-boundary conditions for the V_h potential on the sides. In this case, the planar circuit methods may be applied to a guide with changing height.

As shown, all the cases for planar circuits lead to a set of equations (6) and (7) or (8) and (9) which may be written in a standard form

$$\nabla V(x, y) = -j\omega L_s\boldsymbol{J}(x, y) \tag{11}$$

$$\nabla\cdot\boldsymbol{J}(x, y) = -j\omega C_s V(x, y). \tag{12}$$

We shall now concentrate on the E_0 mode. It does not mean that the formulas presented in the next section are invalid for the higher modes. They are valid, but their physical interpretations are more complicated and will not be considered here.

For the mode E_0, the value C_s is the capacitance of a unitary square of the circuit, and the value of L_s is the inductance of an arbitrary square of the circuit.

III. The Proposed Method of Analysis

The proposed method of analysis is based on the finite-difference method [6], [7]. Let us consider (11) and (12) in the time-dependent form

$$\nabla V(x, y, t) = -L_s\frac{\partial\boldsymbol{J}(x, y, t)}{\partial t} \tag{13}$$

$$\nabla\cdot\boldsymbol{J}(x, y, t) = -C_s\frac{\partial V(x, y, t)}{\partial t}. \tag{14}$$

The xy-plane (the domain of the functions V and $\boldsymbol{J}$) is divided into a set of square meshes of the size a. The coordinates of the middle of a mesh in the kth row and the lth column are denoted by x_l and y_k. Let us assume that (13) and (14) describe propagation of a wave of the frequency ω and the wavelength λ. If we assume that $a \ll \lambda$ and $\Delta t \ll \frac{2\pi}{\omega}$, we may replace the differentials in (13) and (14) by finite differences Δt and a. After algebraic transformations, we obtain the relations for V and two components of the current J_x and J_y inside the circuit

$$J_x\left(x_l + \frac{a}{2}, y_k, t_0 + \frac{\Delta t}{2}\right) = J_x\left(x_l + \frac{a}{2}, y_k, t_0 - \frac{\Delta t}{2}\right) - \left(V(x_l + a, y_k, t_0) - V(x_l, y_k, t_0)\right)\frac{\Delta t}{L_s a} \tag{15}$$

$$J_y\left(x_l, y_k + \frac{a}{2}, t_0 + \frac{\Delta t}{2}\right) = J_y\left(x_l, y_k + \frac{a}{2}, t_0 - \frac{\Delta t}{2}\right) - \left(V(x_l, y_k + a, t_0) - V(x_l, y_k, t_0)\right)\frac{\Delta t}{L_s a} \tag{16}$$

$$V(x_l, y_k, t_0 + \Delta t) = V(x_l, y_k, t_0) + \left(J_x\left(x_l + \frac{a}{2}, y_k, t_0 + \frac{\Delta t}{2}\right) - J_x\left(x_l - \frac{a}{2}, y_k, t_0 + \frac{\Delta t}{2}\right) + J_y\left(x_l, y_k + \frac{a}{2}, t_0 + \frac{\Delta t}{2}\right) - J_y\left(x_l, y_k - \frac{a}{2}, t_0 + \frac{\Delta t}{2}\right)\right)\frac{\Delta t}{C_s a}. \tag{17}$$

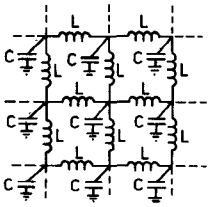

Fig. 2. Lumped circuit equivalent to a segment of a planar circuit.

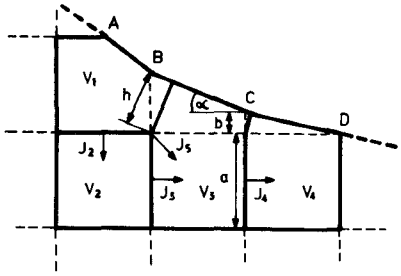

Fig. 3. Example of an open boundary approximation.

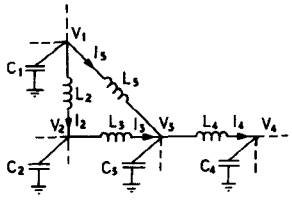

Fig. 4. Lumped circuit equivalent to the circuit considered in Fig. 3.

Equations (15)–(17) describing the circuit have an interesting interpretation. The circuit may be represented as a set of lumped capacitors C and inductances L, as presented in Fig. 2. The potential V has the meaning of the voltage. The current flowing in the inductances may be calculated as $I_x = J_x a$ and $I_y = J_y a$. The elements values are $C = C_s a^2$, $L = L_s$.

A. Boundary Conditions

If a short-circuited border line passes through the centers of the meshes in one column or one row, the boundary conditions are satisfied by assuming $V = 0$ at those points. If an open-circuited border line follows a side line of a row or a column of meshes, the boundary conditions are satisfied by putting $J_n = 0$, where J_n is the current density component perpendicular to the border line.

Those simple rules are sufficient to calculate a circuit of a rectangular shape, but if we want to analyze an arbitrarily-shaped circuit without significant loss of accuracy, a procedure conforming the boundary shape is needed. That kind of procedure for an open boundary will be introduced using an example of a segment of a circuit shown in Fig. 3, and its equivalent LC circuit shown in Fig. 4. The border line was approximated by a broken line $ABCD$. Four meshes close to the border are considered and the potentials in the centers of them are denoted by $V_1 \cdots V_4$.

To match the border line, the meshes 1, 3, and 4 are deformed as shown in Fig. 3. In the neighborhood of the border, they are limited by the line $ABCD$ or by perpendiculars dropped on it from the nodal points. Since (14) may be written in an integral form

$$\oint_{L_m} \boldsymbol{J} \cdot \boldsymbol{a}_n \, dl = -C_s \int_{S_m} \frac{\partial V}{\partial t} \, ds \simeq -C_s S_m \frac{dV_m}{dt} \tag{18}$$

where S_m is the surface of the mth mesh, a_n is the unit vector perpendicular to L_m, L_m-border line of the mth mesh, and the capacitances C_1, C_2, and C_4 in the equivalent circuit in Fig. 4 are proportional to the surfaces of the corresponding meshes.

The inductances L_2 and L_3 are the standard inductances between meshes $L_2 = L_3 = L_s$.

To calculate L_4, we note that

$$\frac{dJ_4}{dt} \simeq -\frac{V_4 - V_3}{aL_s}$$

and that the current passing between the meshes 3 and 4 is equal to

$$I_4 \simeq J_4(a+b). \tag{19}$$

Thus

$$-\frac{V_4 - V_3}{L_4} = \frac{dI_4}{dt} \simeq -\frac{(V_4 - V_3)}{L_s} \frac{(a+b)}{a}$$

or

$$L_4 \simeq L_s \frac{a}{a+b}. \tag{20}$$

To calculate L_5, we put

$$\frac{dJ_5}{dt} \simeq \frac{V_3 - V_1}{L_s a\sqrt{2}}.$$

Since near the open boundary there exist only a tangential component of the current

$$I_5 \simeq \frac{J_5 h}{\cos\left(\frac{\pi}{4} - \alpha\right)} \tag{21}$$

which gives

$$-\frac{V_3 - V_1}{L_5} = \frac{dI_5}{dt} \simeq -\frac{h}{\cos\left(\frac{\pi}{4} - \alpha\right)} \frac{V_3 - V_1}{L_s a\sqrt{2}}$$

and

$$L_5 \simeq L_s \frac{a\sqrt{2}\cos\left(\frac{\pi}{4} - \alpha\right)}{h}. \tag{22}$$

B. Lumped Elements in the Circuit

Direct correspondence between the algorithm used for calculation and the equivalent LC circuit makes it easy to consider lumped elements branched into the circuit. These elements may be passive (R, L, C) or active (voltage or current sources), and, since a time-domain method is used, they may be nonlinear. It should be noted, however, that (15)–(17) describe the voltages at the points of time and space different from those where and when the currents are described. The differences are $\Delta t/2$ in time and $a/2$ in

space and they should be considered to avoid errors in impedance calculations.

C. Algorithm Stability

A computer algorithm based on (15)–(17), with excitation by a set of sinusoidal sources of a frequency ω, has an important condition of stability. This condition will be introduced through its physical interpretation.

In the circuit considered, any perturbation of V or J propagates with the velocity of

$$V_g = \frac{d\omega}{d\beta} = \frac{\lambda}{T} \tag{23}$$

where λ is the wavelength of the wave in the planar circuit, and

$$T = \frac{2\pi}{\omega}.$$

In the algorithm after a time Δt, the perturbation reaches the adjacent mesh. It requires $2\Delta t$ to transmit the perturbation from the mesh k, l to the mesh $k+1, l+1$. Thus, the velocity of propagation in the algorithm is not smaller than

$$V_a = \frac{a\sqrt{2}}{2\Delta t}. \tag{24}$$

To assure the proper functioning of the algorithm we must have

$$V_a > V_g$$

or

$$\frac{a}{\sqrt{2}\lambda} > \frac{\Delta t}{T}. \tag{25}$$

The same result may be obtained from the theory of finite-difference methods (see [6, sec. 26.2]).

D. Accuracy of the Calculations

There are three principal causes of errors in the proposed numerical method of planar-circuit analysis.

1) replacing the differential equations (13) and (14) by (15), (16), and (17),
2) approximation of the circuit border line, and
3) assumption of a steady state in the circuit after a finite period of time.

To analyze the first cause of errors, let us consider, for example, (15). To obtain it from (13), we have replaced the differentials by finite differences. Since some error of this replacement exists, we may write

$$\frac{\partial J_x\left(x_l + \frac{a}{2}, y_k, t_0\right)}{t} = \frac{J_x\left(x_l + \frac{a}{2}, y_k, t_0 + \frac{\Delta t}{2}\right) - J_x\left(x_l + \frac{a}{2}, y_k, t_0 - \frac{\Delta t}{2}\right)}{\Delta t} + \delta_{Jx} \tag{26}$$

$$\frac{\partial V\left(x_l + \frac{a}{2}, y_k, t_0\right)}{\partial x} = \frac{V(x_l + a, y_k, t_0) - V(x_l, y_k, t_0)}{a} + \delta_V. \tag{27}$$

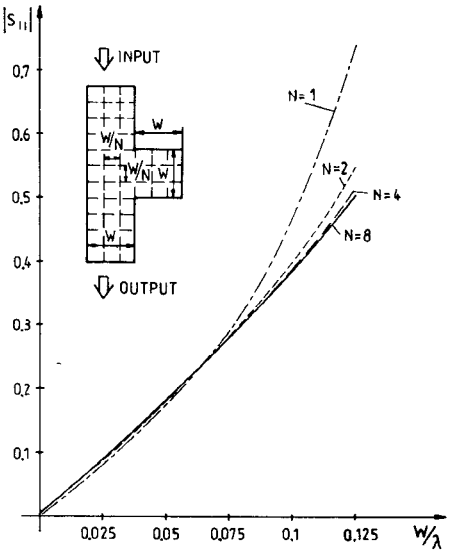

Fig. 5. Comparison of the results of calculation for different mesh size $a = \frac{w}{N}$.

Development of the functions V and J_x in Taylor series gives

$$\delta_{Jx} = \frac{\partial^3 J_x\left(x_l + \frac{a}{2}, y_k, t_0\right)}{\partial t^3} \frac{\Delta t^2}{24} + \cdots \tag{28}$$

$$\delta_V = \frac{\partial^3 V\left(x_l + \frac{a}{2}, y_k, t_0\right)}{\partial x^3} \frac{a^2}{24} + \cdots. \tag{29}$$

From (28) and (29), it is seen that the errors are proportional to Δt^2 or a^2. This means that the errors decrease rapidly with a decrease in the mesh size and a decrease in the size of a step in time.

Since the values of Δt and a are bound by the condition (25), the error caused by the approximation of the function of time has a minor effect. The value of δ_V and similar values of errors found in the analysis of (16) and (17) depend on the field distribution in the circuit. Typically, the functions $V(x, y)$ and $J(x, y)$ change slowly in space following a sinusoidal-type distribution over a wavelength. Thus, the third derivatives of these functions are not very big and the errors are small even for relatively high values of a. An example of this is shown in Fig. 5, where the results are displayed for different sizes of the meshes assumed for calculations. Nevertheless, if the boundary conditions force rapid changes of $V(x, y)$ and $J(x, y)$, the third derivatives of these functions may cause some increase in the errors.

It is difficult to obtain mathematical approximations for the other two causes of errors. We may formulate only some general remarks. The second cause of errors obviously depends on the possibility of reasonable approximation of the boundary line by a straight line within one mesh. The experiments have confirmed that if such an approximation is possible, the error introduced by approximating the shape of the boundary does not have a dominating role in the total error of calculations.

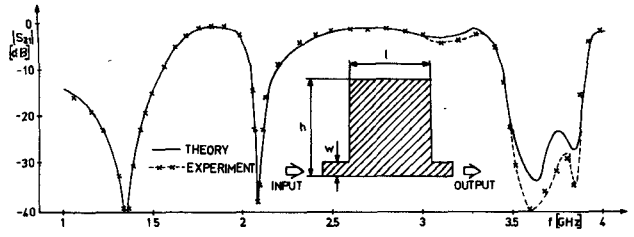

Fig. 6. $|S_{21}|$ of a rectangular stripline circuit calculated and measured in the 1–4-GHz band.

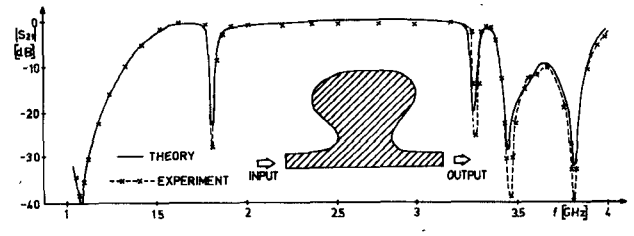

Fig. 7. $|S_{21}|$ of a stripline circuit of irregular shape calculated and measured in the 1–4-GHz band.

The time needed to stabilize the oscillations in the circuit may be assumed by the user taking into account the circuit dimensions and its loaded Q-factor. Another possibility is to leave the time of terminating the calculations to be set up automatically in the algorithm on the basis of the shape of the $V(t)$ function monitored in several chosen points of the circuit. It is always possible to reduce the error caused by a transient response to a negligible value, but it is very time consuming for the circuits of a high loaded Q-factor.

E. Examples of Application

Figs. 6 and 7 show the comparison of the calculated and measured values of $|S_{21}|$ as a function of the frequency in 1–4-GHz band for two stripline circuits. The shape of the inner strip of each circuit is also presented. Both circuits were built on a stripline of the height $2d = 6.94$ mm filled with a dielectric of $\epsilon_r = 2.5$.

The dimensions of the circuit in Fig. 6 are $w = 5.2$ mm, $l = 46.5$ mm, and $h = 54.8$ mm. The fringing fields were included in the calculations by increasing these dimensions according to (10) to the values $w' = 8.27$ mm, $l' = 49.6$ mm, and $h' = 57.9$ mm. This circuit was designed to be matched exactly by a set of squares of the size $a = \frac{1}{3}w'$. The results of the calculations are in good agreement with those of the measurements. The difference between them visible for higher frequencies may be attributed to higher value of the ratio a/λ. For example, let us assume the frequency $f = 4$ GHz ($a/\lambda = 1/17$) and calculate the error described by (29) assuming a sinusoidal distribution of $V(x, y)$ along the x-axis. We obtain the error at the level of about 45 dB, and, since several similar errors accumulate, the error level of about 30 dB is what we may expect.

Fig. 7 shows the results similar to those of Fig. 6 but obtained for a circuit of a shape drawn at random (which is also shown in Fig. 7). The mesh size assumed for calculations is the same as in the previous example. There is no visible loss of accuracy of the calculations due to an irregular boundary.

F. Computer Memory and Time Needed for Calculation

The method may be implemented on a wide range of computers, including small personal computers. 64 kB of RAM should be sufficient to calculate circuits with 50×50 rectangular elements. The time depends strongly on the number of meshes and also on the period of time required to stabilize the oscillations in the circuit. For example, analyzing the circuit of Fig. 7 for a fixed frequency takes about 1 min in Fortran on a CDC computer of the Cyber 70 series or about 80 min in Pascal on a standard personal computer.

IV. Conclusion

The method presented in this paper shows many advantages.

1) It is very versatile. A universal program may be worked out for an analysis of a planar circuit of any shape defined by the user.

2) The accuracy of calculations can be made sufficient to assure a very good agreement between the theory and the experiment.

3) There are possibilities for the further development of the method. For example, the circuit losses may be easily included in the calculations. It is also possible to analyze a circuit with lumped elements (both linear and nonlinear) branched into it.

4) The method simulates a natural process of the wave propagation, and the actual field distribution may be displayed during the calculations. This may help in debugging the program.

It may also give some valuable information to the circuit designer trying to understand better the physical properties of his circuit. It may also be useful in the teaching of microwaves.

A disadvantage of the method is the long computing time. This is especially important for the circuits of high loaded Q-factors. We may assume, however, that this is the price paid for the mentioned advantages, which may have crucial significance in many applications. We may also assume that due to constant improvement in the speed of computers, the future user will be more willing to pay that price.

References

[1] T. Okoshi and T. Miyoshi, "The planar circuit—An approach to microwave integrated circuitry," *IEEE Trans. Microwave Theory Tech.*, vol. MTT-20, pp. 245–252, Apr. 1972.

[2] Hsu Jui-Pang and T. Anada, "Planar circuit equation and its practical application to planar-type transmission-line circuit," in *IEEE MTT Int. Symp. Dig.* (Boston) 1983, pp. 574–576.

[3] R. Chadha and K. C. Gupta, "Green's functions for triangular segments in planar microwave circuits," *IEEE Trans. Microwave Theory Tech.*, vol. MTT-28 pp. 1139–1143, Oct. 1980.

[4] T. Okoshi, Y. Uehara, and T. Takeuchi, "The segmentation method —An approach to the analysis of microwave planar circuits," *IEEE Trans. Microwave Theory Tech.*, vol. MTT-24, pp. 662–668, Oct. 1976.

[5] R. E. Collin, *Field Theory of Guided Waves*. McGraw-Hill, 1960, chs. 1 and 5.

[6] G. E. Forsythe and W. R. Wasow, *Finite-Difference Methods for Partial Differential Equations*. New York: Wiley, 1960.
[7] G. D. Smith, *Numerical Solution of Partial Differential Equations*. London: Oxford University Press, 1975.

✠

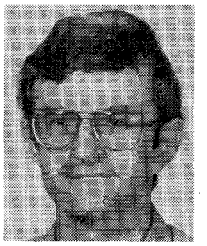

Wojciech K. Gwarek was born in Skarżysko-Kamienna, Poland, on September 13, 1947. He received the M.Sc. (Honors) and Ph.D. degrees in electronic engineering from the Technical University of Warsaw, Warsaw, Poland, in 1970 and 1977, respectively.

Since 1970, he has been with the Institute of Radioelectronics, Technical University of Warsaw, where he is currently a Deputy Director. While on leave during the academic year 1973–1974, he completed the postgraduate study and received the M.Sc. degree from the Massachusetts Institute of Technology, Cambridge, MA, in 1974. His research interests are in the areas of electromagnetic field theory, microwave measurements, and computer-aided analysis of microwave circuits.